Thin Solid Films 517 (2009) 3721–3725

Contents lists available at ScienceDirect

Thin Solid Films

journal homepage: www.elsevier.com/locate/tsf

Structure and optical properties of ZnO:V thin films with different doping concentrations

Liwei Wang [a,b,c], Lijian Meng [a,b,*], Vasco Teixeira [b], Shigeng Song [d], Zheng Xu [c], Xurong Xu [c]

[a] Departamento de Física, Instituto Superior de Engenharia do Porto, Rua Dr. António Bernardino de Almeida 431, 4200-072 Porto, Portugal
[b] Centro de Física, Universidade do Minho, Campus de Azurem, 4800-058 Guimarães, Portugal
[c] Institute of Optoelectronics Technology, Beijing Jiaotong University; Key Laboratory of Luminescence and Optical Information (Beijing Jiaotong University), Ministry of Education, Beijing 100044, China
[d] Thin Film Center, University of Paisley, Paisley PA1 2BE, Scotland, United Kingdom

ARTICLE INFO

Article history:
Received 2 January 2008
Received in revised form 5 December 2008
Accepted 16 December 2008
Available online 25 December 2008

Keywords:
V-doped ZnO
Magnetron sputtering
Optical properties

ABSTRACT

A series of ZnO thin films doped with various vanadium concentrations were prepared on glass substrates by direct current reactive magnetron sputtering. The results of the X-ray diffraction (XRD) show that the films with doping concentration less than 10 at.% have a wurtzite structure and grow mainly along the *c*-axis orientation. The residual stress, estimated by fitting the XRD diffraction peaks, increases with the doping concentration and the grain size also has been calculated from the XRD results, decreases with increasing the doping concentration. The surface morphology of the ZnO:V thin films was examined by SEM. The optical constants (refractive index and extinction coefficient) and the film thickness have been obtained by fitting the transmittance. The optical band gap changed from 3.12 eV to 3.60 eV as doping concentration increased from 1.8 at.% to 13 at.% mol. All the results have been discussed in relation with doping concentration.

1. Introduction

Diluted magnetic semiconductors (DMSs) are a new kind of materials for spintronic application. To be largely used in electronic applications, a spintronic device requires the realization of a ferromagnetic material that exhibits polarized spin density at the carrier bands at room temperature. In DMS materials, transition metal(TM) or rare earth metal ions are substituted onto cation sites of the host semiconductor and coupled with free carriers to introduce ferromagnetism [1]. Dielt et al. [2] and K. Sato et al. [3] have predicted that among the DMS, ZnO doped with transition metal impurities is one of the most promising spintronic materials. There is considerable interest in the development of zinc oxide based (ZnO:TM) diluted magnetic semiconductors because of their high Curie temperature which is essential for spintronic devices [2]. A number of experiments have revealed magnetic properties of ZnO thin films doped with transition metal at room temperature [4–7]. ZnO thin films can be deposited by several physical and chemical deposition techniques, such as laser-molecular-beam-epitaxy [8], chemical vapor deposition [9], pulsed laser deposition [10] and sputtering [11]. Among these depositing techniques, sputtering technique presents some important advantages and improved technological possibilities [12–14].

Sputtering technique, which requires less expensive setup, is quite simple and is considered to be the most favorable deposition method to obtain highly uniform films which have high packing density and strong adhesion at a high deposition rate [15]. In this paper, a series of ZnO thin films doped with various vanadium concentrations were prepared by direct current(DC) reactive magnetron sputtering and the structure and optical properties of ZnO:V films were analyzed in detailed.

2. Experiment

ZnO:V thin films were deposited on the glass substrate by DC magnetron sputtering using zinc (99.99%) metal target with some pieces of vanadium sticking on the surface of the target. The distance between the target and the substrate was 50 mm. The sputtering chamber was evacuated to a base pressure below $3*10^{-3}$ Pa before argon gas. After vacuum pumping, the sputtering gas Ar with a purity of 99.99% and the reactive gas O_2 with a purity of 99.99% were introduced into the chamber separately and controlled by the standard mass flow controllers. The total pressure and the oxygen partial pressure were kept at 0.9 Pa and 0.3 Pa, respectively and the sputtering current was fixed at 0.3 A. The substrate was without extra hearting.

The structure and crystallinity of the films were investigated by X-ray diffraction (XRD) (Philips PW-1710 with Cu Kα radiation λ = 0.154056 nm, 40 kV, 30 mA) measurements, which scan range from 10° to 80° using 0.02 degree steps. The surface morphologies of the films were monitored

* Corresponding author. Departamento de Física, Instituto Superior de Engenharia do Porto, Rua Dr. António Bernardino de Almeida 431, 4200-072 Porto, Portugal. Tel.: +351962325429; fax: +351228321159.
E-mail address: ljm@isep.ipp.pt (L. Meng).

0040-6090/$ – see front matter © 2008 Elsevier B.V. All rights reserved.
doi:10.1016/j.tsf.2008.12.043

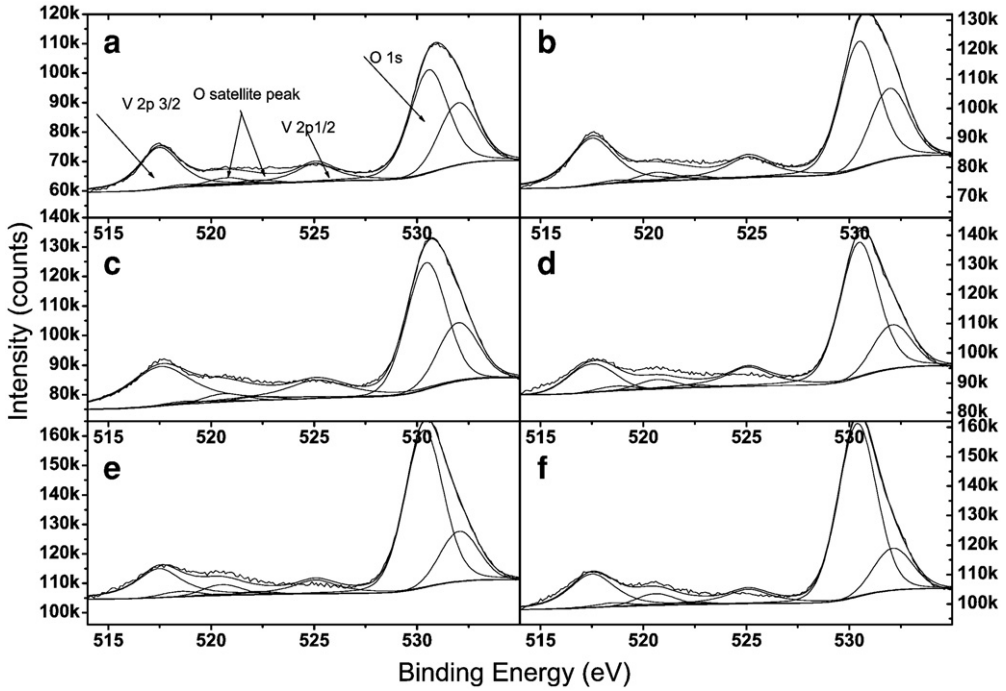

Fig. 1. XPS of ZnO:V film with different concentrations (a) 13 at.%, (b) 10 at.%, (c) 6.8 at.%, (d) 5.8 at.%, (e) 3.9 at.%, and (f) 1.8 at.%.

by field emission scanning electron microscope (FESEM) (Joel JSM 6301F, 15 kV) and the stoichiometries of the films were determined by Energy Dispersive X-ray Spectroscopy (EDS) (Oxford INCA 350 Energy) with 15 kV collected for 50 s and using EDAX PhiRhoZ Quantification to analyze the stoichiometries. X-ray photoelectronic spectrometry (XPS) data were recorded on a VG ESCALAB using an AlKa line radiation source (with a base pressure of 10^{-7} Pa, 15 kV, 20 mA). Region characteristics for signals were run in high resolution mode using 0.1 eV steps and calibrated the binding energy by C 1s at 285 eV. The charge state of V ions in the ZnO:V films was characterized by XPS. The optical properties were characterized by transmittance spectra measured using a Shimadzu UV-3101PC spectrophotometer at 300–2500 nm. The film thickness was valued with FESEM and calculated from the transmittance.

3. Results and discussion

Vanadium concentration in ZnO films was detected by EDS measurements. The doping concentration is varied from 1.8 at.% to 13 at.%. In order to analyze the chemical states of the constituent elements, XPS measurements were performed with an emphasis on the peaks associated with Zn_{2p}, V_{2p}, and O_{1s}. Fig. 1 presents the V 2p core-level photoemission spectrum. The charge shifted spectra were corrected using the adventitious C 1s photoelectron signal at 285 eV. It is clear from Fig. 1 that the V $2p_{3/2}$ core levels for V–O bonding were situated at 517.5 eV, and the energy difference between V $2p_{3/2}$ and V $2p_{1/2}$ was 7.6 eV [16]. This suggests that the V ions in the films are in the chemical state of V^{5+}. Besides, XPS data showed that no V clusters existed in the ZnO:V thin films.

Fig. 2 gives the deposition rate of ZnO thin films with different doping concentrations. The total pressure and the oxygen partial pressure were kept at 0.9 Pa and 0.3 Pa respectively at fixed current 0.3 A. The deposition time is 25 min. The deposition rate decreases as the doping concentration increases. It may result from the difference of the sputtering yield for vanadium and zinc. Chapman [17] gives an equation of reactive sputtering yield as follows:

$$Y = \frac{3\alpha m_i m_t E}{\pi^2 E_0 (m_i + m_t)^2} \quad (1)$$

where E_0 is the binding energy of the surface atoms, m_i and m_t are masses of incident atom and the target atom respectively, E is the

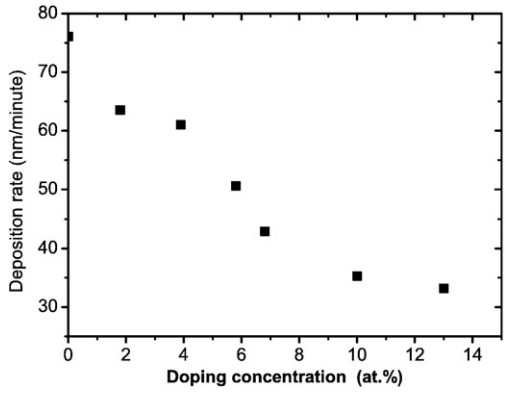

Fig. 2. Deposition rate at different doping concentrations.

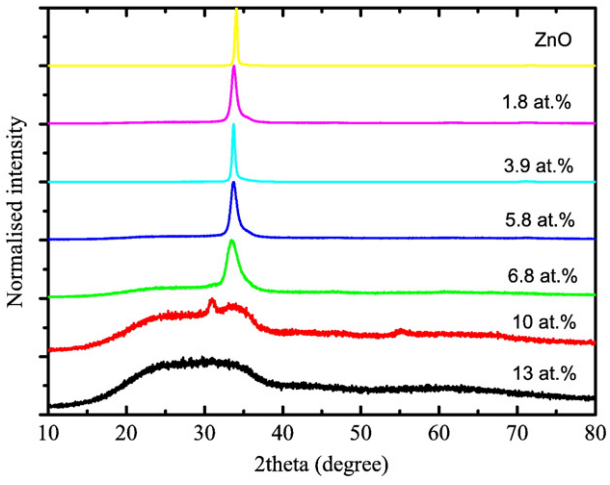

Fig. 3. XRD patterns of ZnO:V films with various doping concentrations.

Table 1
Grain size along (001) direction and residual stress of the ZnO:V films with various concentrations prepared with different doping concentrations.

Doping concentration	d (A)	Stress (GPa)	FWHM	Grain size (nm)	Thickness (nm)
13 at.%					664
10 at.%					706
6.8 at.%	2.678	−6.69	1.66	5.0	859
5.8 at.%	2.660	−5.03	0.88	9.5	1012
3.9 at.%	2.656	−4.69	0.71	11.7	1220
1.8 at.%	2.658	−4.89	0.40	20.8	1271
0 at.%	2.633	−2.72	0.31	27.4	1522

energy of the incident atom. α is a function of m_t/m_i and it increases with the value of m_t/m_i. $\frac{m_i m_t}{(m_i + m_t)^2}$ increases a little from zinc to vanadium, but $\frac{3\alpha E}{\pi^2 E_0}$ decreases a lot from zinc to vanadium. According to Eq. (1), the sputtering yield of zinc is much bigger than that of vanadium.

3.1. Structural properties

Fig. 3 shows the XRD patterns of ZnO:V thin film doped with various vanadium concentrations. It shows that the films with the doping concentration below 6.8 at.% have a preferred orientation along the (001) direction. ZnO:V thin films below 6.8 at.% have a preferential c-axis orientation. The doping concentration further arrives to 10 at.%, the (002) peak of ZnO disappeared and another peak were observed at $2\theta = 30$ corresponding to ZnO (100). However, when the doping concentration goes up to 13 at.%, the film shows an amorphous structure. This indicates that higher content of vanadium leads to a deterioration of the crystal structure by distorting the ZnO lattice. The doping concentration should be lower than 10 at.% in order to get the polycrystalline ZnO thin films.

The full width half maximum (FWHM) of (002) peak was found to increase continuously with the doping concentration. Assuming a homogeneous strain across crystallites, the grain size, representing the longitudinal coherence length in the direction perpendicular to the substrate, is deduced from the (002) peak width by using the Debye–Scherrer's formula [18]

$$D = \frac{0.9\lambda}{B\cos\theta} \tag{2}$$

where D is the grain size, λ is the X-ray wavelength, θ is the Bragg diffraction angle and B is the full width half maximum (FWHM) of the diffraction peak. By fitting the XRD results, the average grain size of the films has been calculated from the (002) diffraction peak. The calculated grain sizes with lower doping concentration are shown in Table 1. It can be found that the grain size decreases with the increase of vanadium concentration. The broadening in X-ray peak with an increase of vanadium concentration is observed which indicates the deteriorated effect of vanadium on ZnO crystalline quality. This confirms that the disordering increases with the increase of vanadium concentration in ZnO thin films. It is reported that the incorporation of 3d transition metal deteriorates generally the crystallinity of ZnO [1]. It may due to the vanadium ions that could disturb the ZnO crystal lattice and obstruct the crystal growth. Z.C. Chen et al. have reported similar result in ZnO:Fe [19].

The positions of (002) peak are given in Table 1. It can be seen that the position of (002) peak shifted to lower angles gradually with the increasing of doping concentration until 6.8 at.%. It is important to note that the value of the c-axis lattice parameter for the ZnO:V films is larger than the standard value of 5.2066 Å. The residual stresses of the films are calculated from the value of lattice parameter of film by Eq. (3) [20]

$$\sigma = \frac{2c_{13}^2 - c_{33}(c_{11} + c_{12})}{2c_{13}} \frac{d - d_0}{d_0} \tag{3}$$

where d is the crystallite plane spacing of the films, and $d_0 = 2.6033$ Å is the standard plane spacing from X-ray diffraction. The values of the elastic constant from single crystalline ZnO are used, $c_{11} = 208.8$ GPa, $c_{33} = 213.8$ GPa, $c_{12} = 119.7$ GPa and $c_{13} = 104.2$ GPa. Substituting these values in the above equation gives $\sigma = -233(d - d_0)/d_0$. The calculated

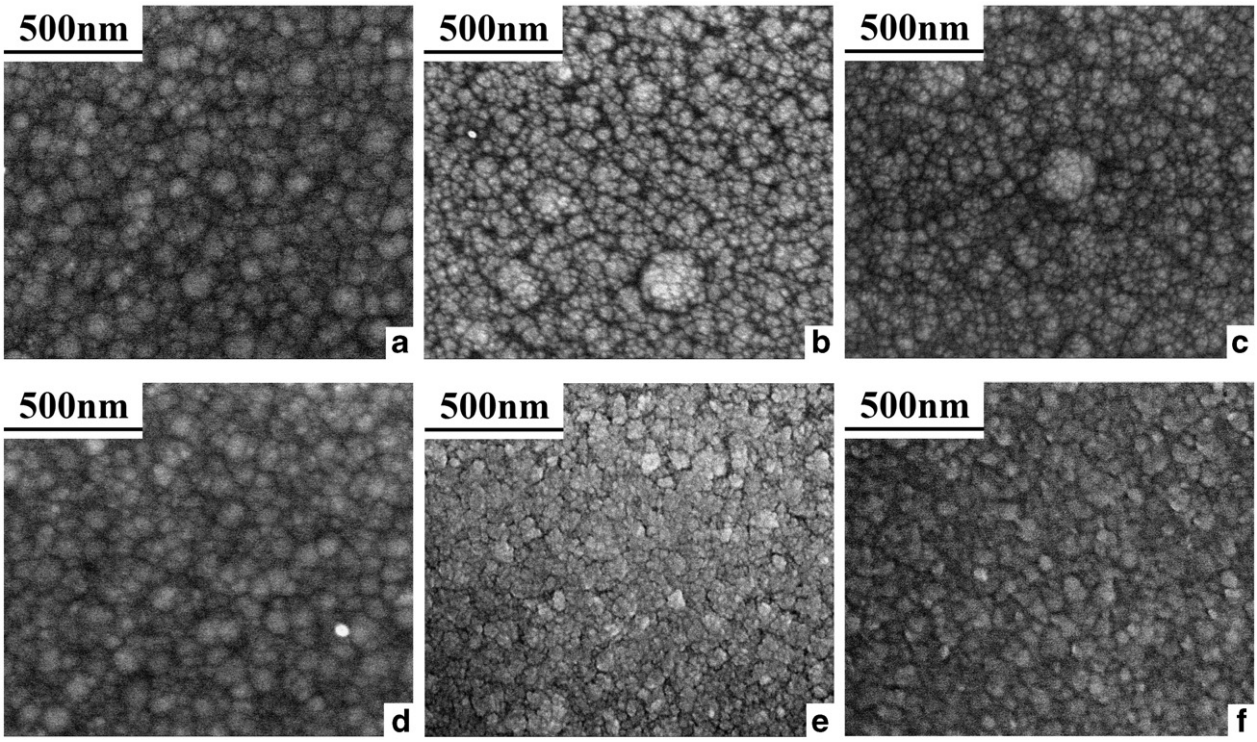

Fig. 4. SEM micrographs of films prepared with various doping concentrations (a) 1.8 at.%, (b) 3.9 at.%, (c) 5.8 at.%, (d) 6.8 at.%, (e) 10 at.%, and (f) 13 at.%.

residual stresses of the films are shown in Table 1. From Table 1 it can be seen that all the samples have a negative residual stress which indicates a compressive stress in the films. The residual stress of the films increases with the increase of doping concentration. Since all the ZnO films with different doping concentrations were grown at room temperature under similar processing condition, the presence of stress is not related to the mismatch in the thermal expansion coefficient with the glass substrate. However, the presence of interstitial oxygen has an expansive effect on the lattice, which results in the compressive strain, normally, occurring along the *c* axis. Therefore, the additive contribution of the presence of interstitial defects and the incorporation of vanadium in ZnO lattice site are responsible for the presence of large stress in the ZnO:V thin films.

3.2. Surface morphology

The surface morphology of the deposited ZnO:V films with various concentrations was examined by FESEM as shown in Fig. 4. It can be seen that the average particle size along the surface and the roughness of the film increases with the increasing of concentration of vanadium. The surface of the films with doping concentration at 10 at.% and 13 at.% are very different from the others. This is in agreement with the XRD result. As we can see, the large doping concentration can destroy the crystal structure.

3.3. Optical properties

Optical transmission spectra of the ZnO:V films in the wavelength region of 300–900 nm are shown in Fig. 5. Transmittance spectra of all samples exhibit interference fringe patterns with an average transmission of 80% indicating the good optical quality of the deposited films. The transmission is found to be the maximum for the film with 13% doping concentration in ZnO film and decreases with the decrease of doping concentration until 3.9 at.%. This may be due to the thickness of the films and the doping effect. The transmittance increases with the doping concentration because of the disorder of the films. The scatter of the amorphous film will be less than the polycrystalline films. The transmittances of thin films with doping concentration below 3.9 at.% decrease with increase of the doping concentration. The decrease in optical transmission with lower concentration is associated with the scattering at grain boundaries. The increase in scattering centers, which is caused by more grain boundaries with an increase in V dopant content, should be responsible for the loss of transmission. The grain size decreases and thereby increase grain boundaries in ZnO:V thin films, which agrees with the results calculated from XRD. The difference in the absorption edge of ZnO:V thin films was observed compared with that of pure ZnO films. A sharp absorption edge was observed for pure ZnO thin film. However, the absorption edge of ZnO:V films shows a broader edge with the increase of doping concentration. The broadening of absorption edge suggests an increase of the disorder in ZnO:V film with incorporation of vanadium, which is in agreement with X-ray diffraction analysis as discussed before. In the present work, the thickness, refractive index and extinction coefficient of films have been obtained by fitting from the transmittance spectra using the Drude model and OJL [S.K. O'Leary, S.R. Johnson, P.K. Lim] model [21,22].

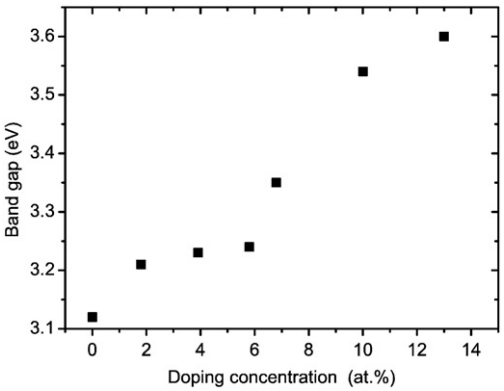

Fig. 6. The band gap dependence on the doping concentration.

In order to model the inter-band transitions, we have used two models to generate theoretical spectra for the transmittance of thin ZnO:V films in the spectral range from 300 to 2500 nm. In order to get a satisfying fit, the following models were applied:

(a) Drude model with frequency-dependent damping to describe the intra-band transitions of the electrons in the conduction band. The classical Drude model of free charge carriers leads to a simple expression of the susceptibility with only two parameters, the plasma frequency and the damping constant. If the effective mass is known, these quantities can be directly related to the charge carrier density and their mobility [21].

(b) The O'Leary–Johnson–Lim (OJL) model that has been proposed to model the band gap transitions of amorphous materials [22].

3.3.1. Band gap

The energy band gap can be obtained from the simulation model. The optical energy band gap of the films was found to increase from

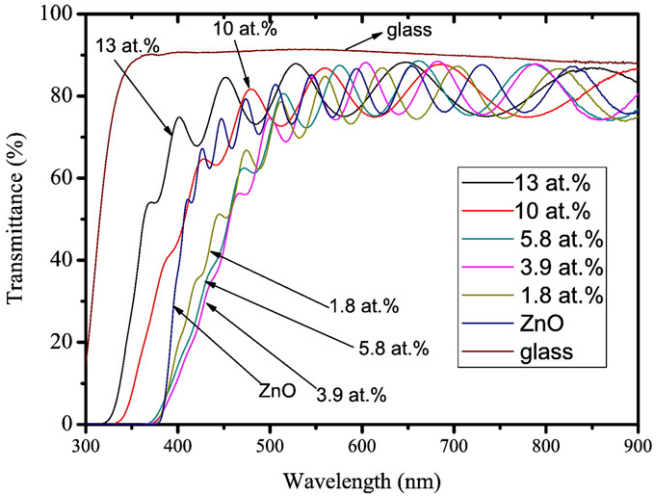

Fig. 5. Optical transmittance spectra of the V doped ZnO films with various doping concentrations.

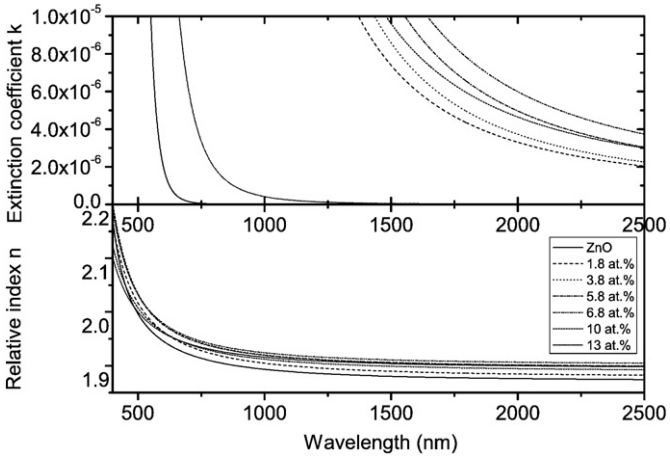

Fig. 7. a) The refractive index and b) the extinction coefficient of the films with different doping concentrations.

3.12 to 3.60 eV with increasing the doping concentration as shown in Fig. 6. These relative high shifts may be due to the influence of several factors such as thickness, grain size, structural parameters and lattice strain, carrier concentration, presence of impurities (or other defects), or even deviation from stoichiometry [23,24]. But for these samples, the reason for the increasing should be mainly thickness and doping concentration.

3.3.2. Refractive index and extinction coefficient

Refractive index of a transparent DMS is an important parameter for magneto-optical device design such as magneto-optical isolators and modulators. The variation of refractive index varies with the photon energy for all the films and is shown in Fig. 7(a). The refractive index of the samples increases with the doping concentration below 6.8 at.% and then decreases. The increase in refractive index is attributed to the decreasing in the value of grain size with the vanadium doping concentration. The decreasing of the transmittance is from the poor qualities of the films. But for all of the doped ZnO, the refractive index is bigger than pure ZnO thin film in the same deposition condition. The observed variation of refractive index with doping concentration for ZnO:V films can be explained on the basis of the contribution from both lattice contraction and the disorder of the films. Generally, dense thin films with optical and structural homogeneity are desirable for industrial applications, since stability and reproducibility of optical and electrical properties are strictly related to the density of atoms per unit volume. The *n* values are dependent on the density of the atoms in the UV–vis spectral range. So the doping concentration needs to be below 6.8 at.%. These results agree with the XRD result.

From Fig. 7(b), the extinction coefficient of films shows similar dependence on wavelength to the refractive index.

4. Conclusion

In summary, ZnO:V films were prepared with various concentrations (0 at.%, 1.8 at.%, 3.9 at.%, 5.8 at.%, 6.8 at.%, 10 at.% and 13 at.%) on glass substrates using the DC magnetron sputtering technique and the properties were discussed from the effect of various vanadium concentrations on the structure, morphology and optical properties of ZnO:V films in details. From the XRD patterns of ZnO:V films, the samples had a preferential *c*-axis orientation and the position of (002) peak with the doping concentration below 6.8 at.%. At the concentration 10 at.%, a peak (002) of ZnO disappeared and a weak peak (100) of ZnO exists. At the doping concentration of 13 at.%, the film becomes amorphous. High dopant concentration hinders crystallization. The SEM images showed the surface topography of the deposited ZnO:V films. The transmittance of the ZnO:V thin films decreases with decreasing the doping concentration until 3.9 at.% and then increases. The thickness, refractive index and extinction coefficient of films have been obtained by fitting from the transmittance spectra using the Drude model and OJL model. The refractive index of the samples increases with the doping concentration below 6.8 at.% and then decreases but the refractive index of all the doped samples is bigger than pure ZnO, which is due to the lattice contraction and the disorder of the films. The extinction coefficient of films has similar dependence on the wavelength.

Acknowledgments

The authors express their thanks to the NSFC (60576016 and 10774013), 863 program (2006AA03Z0412), BNSFC (2073030), 973 Program (2003CB314707), Key program of NSFC(10434030) and FBJTU (2005SM057 and 2006XM043) and Beijing Jiao Tong University Doctor Science Creative Grants No. 48027.

References

[1] S.J. Pearton, D.P. Norton, K. Ip, Y.W. Heo, T. Steiner, J. Vac. Sci. Technol. B 22 (2004) 932.
[2] T. Dietl, H. Ohno, F. Matsukura, J. Cibert, D. Ferrand, Science 287 (2000) 1019.
[3] K. Sato, H. Katayama-Yoshida, Jpn. J. Appl. Phys Part 2 Lett. 39 (2000) L555.
[4] M. Diaconu, H. Schmidt, H. Hochmuth, M. Lorenz, G. Benndorf, J. Lenzner, D. Spemann, A. Setzer, K.W. Nielsen, P. Esquinazi, M. Grundmann, Thin Solid Films 486 (2005) 117.
[5] C.H. Choi, S.H. Kim, Thin Solid Films 515 (2007) 2864.
[6] E. Bacaksiz, S. Aksu, B.M. Basol, M. Altunbaş, M. Parlak, E. Yanmaz, Thin Solid Films 516 (2008) 7899.
[7] J.C. Pivin, G. Socol, I. Mihailescu, P. Berthet, F. Singh, M.K. Patel, L. Vincent, Thin Solid Films 517 (2008) 916.
[8] S.J. An, W.I. Park, G.C. Yi, S. Cho, Appl. Phys. A 74 (2002) 509.
[9] T.M. Barnes, J. Leaf, C. Fry, C.A. Wolden, J. Cryst. Growth 274 (2005) 412.
[10] V. Craciun, S. Amirhaghi, D. Craciun, J. Elders, J. Gardeniers, I.W. Boyd, Appl. Surf. Sci. 86 (1995) 99.
[11] D.J. Kang, J.S. Kim, S.W. Jeong, Y. Roh, S.H. Jeong, J.H. Boo, Thin Solid Films 475 (2005) 160.
[12] Z.Z. Ye, J.F. Tang, Appl. Opt. 28 (1989) 2817.
[13] F.J. Zhang, A. Vollmer, J. Zhang, Z. Xu, J.P. Rabe, N. Koch, Org. Electron. 8 (2007) 606.
[14] Q.B. Ma, Z.Z. Ye, H.P. He, J.R. Wang, L.P. Zhu, B.H. Zhao, Mater. Charact. 59 (2008) 124.
[15] Q.B. Ma, Z.Z. Ye, H.P. He, S.H. Hu, J.R. Wang, L.P. Zhu, Y.Z. Zhang, B.H. Zhao, J. Cryst. Growth 304 (2007) 64.
[16] J.F. Moulder, W.F. Stickle, P.E. Sobol, K.D. Bomben, Handbook of X-ray Photoelectron Spectroscopy, Physical Electronics Inc, USA, 1995.
[17] B. Chapman, Sputtering [Glow Discharge Process], John Wiley&Sons Inc, New York, 1980, p. 177.
[18] M.T. Weller, Inorganic Materials Chemistry, Oxford University Press, Oxford, 1997.
[19] Z.C. Chen, L.J. Zhuge, X.M. Wu, Y.D. Meng, Thin Solid Films 515 (2007) 5462.
[20] Y.G. Wang, S.P. Lau, H.W. Lee, S.F. Yu, B.K. Tay, X.H. Zhang, K.Y. Tse, H.H. Hng, J. Appl. Phys. 94 (2003) 1597.
[21] N.W. Ashcroft, N.D. Mermin, Solid State Physics, Saunders Co., Philadelphia, 1976.
[22] S.K. O'Leary, S.R. Johnson, P.K. Lim, J. Appl. Phys. 82 (1997) 3334.
[23] T. Ren, H.R. Baker, K.M. Poduska, Thin Solid Films 515 (2007) 7976.
[24] R.E. Marottia, D.N. Guerraa, C. Bellob, G. Machadoa, E.A. Dalchiele, Sol. Energy Mater. Sol. Cells 82 (2004) 85.